



Transducer Sound Radiation

Learning Objectives

Planar Immersion Transducer

- on-axis near field - far field

- radiation into solid-normal incidence, plane interface

- diffraction correction

Spherically focused transducer

- on axis field

- focal spot size

- radiation into solid-normal incidence, plane interface

- diffraction correction

Learning Objectives (continued)

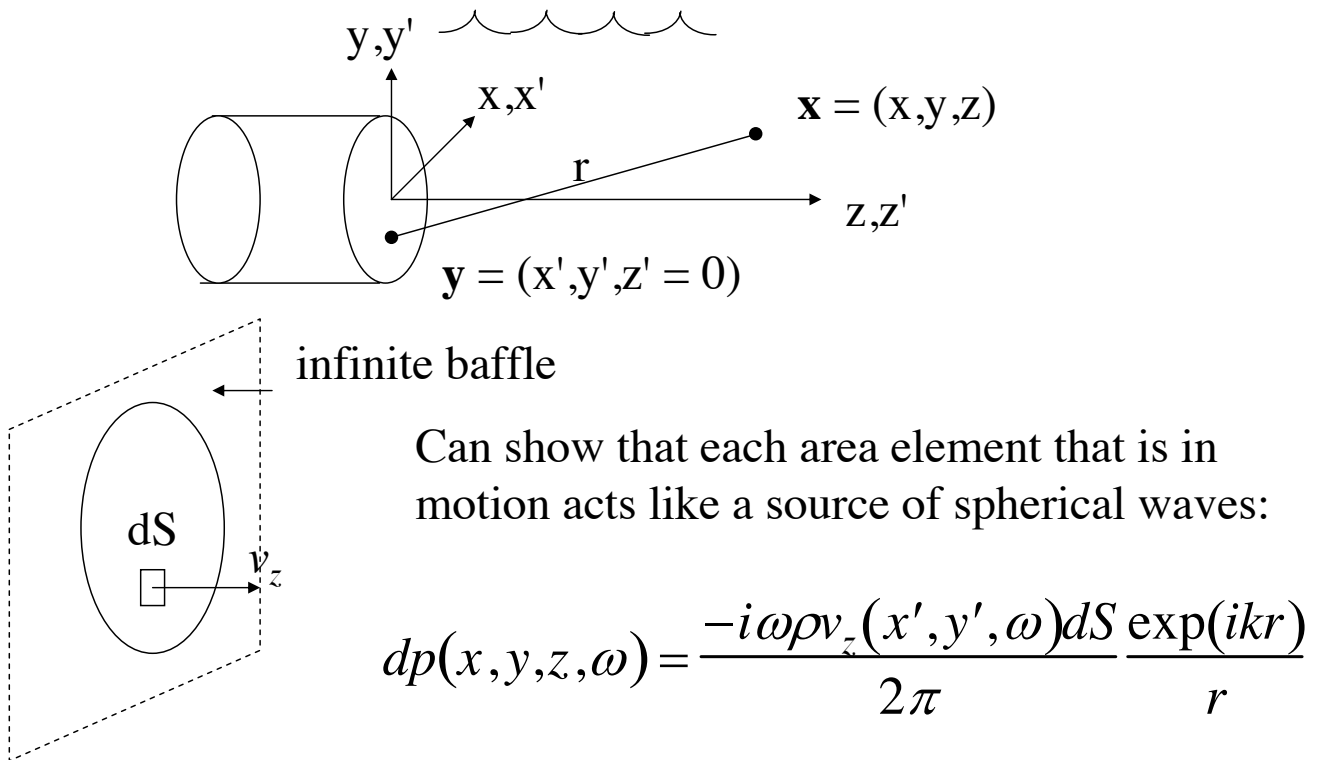
Contact P-wave transducer on a solid
wave types present
directivity functions

Angle beam shear wave transducer

Overview of beam theories

Ultrasonic Beam Models

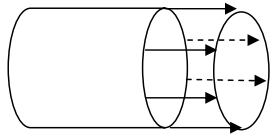
Plane piston transducer radiating into a fluid



Adding up all such sources over the face of the transducer gives the Rayleigh-Sommerfeld Integral

$$p(x, y, z, \omega) = \frac{-i\omega\rho}{2\pi} \int_S \frac{v_z(x', y', \omega) \exp(ikr)}{r} dS(\mathbf{y})$$

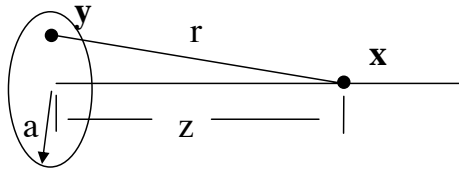
If we let $v_z(x', y', \omega) = v_0(\omega)$ (piston model)



$$\Rightarrow p(x, y, z, \omega) = \frac{-i\omega\rho v_0(\omega)}{2\pi} \int_S \frac{\exp(ikr)}{r} dS(\mathbf{y})$$

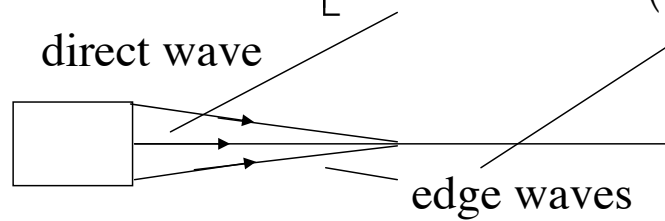
$$p(\mathbf{x}, \omega) = \frac{-i\omega\rho v_0}{2\pi} \int_S \frac{\exp(ikr)}{r} dS(\mathbf{y})$$

For on-axis response of a circular transducer of radius, a

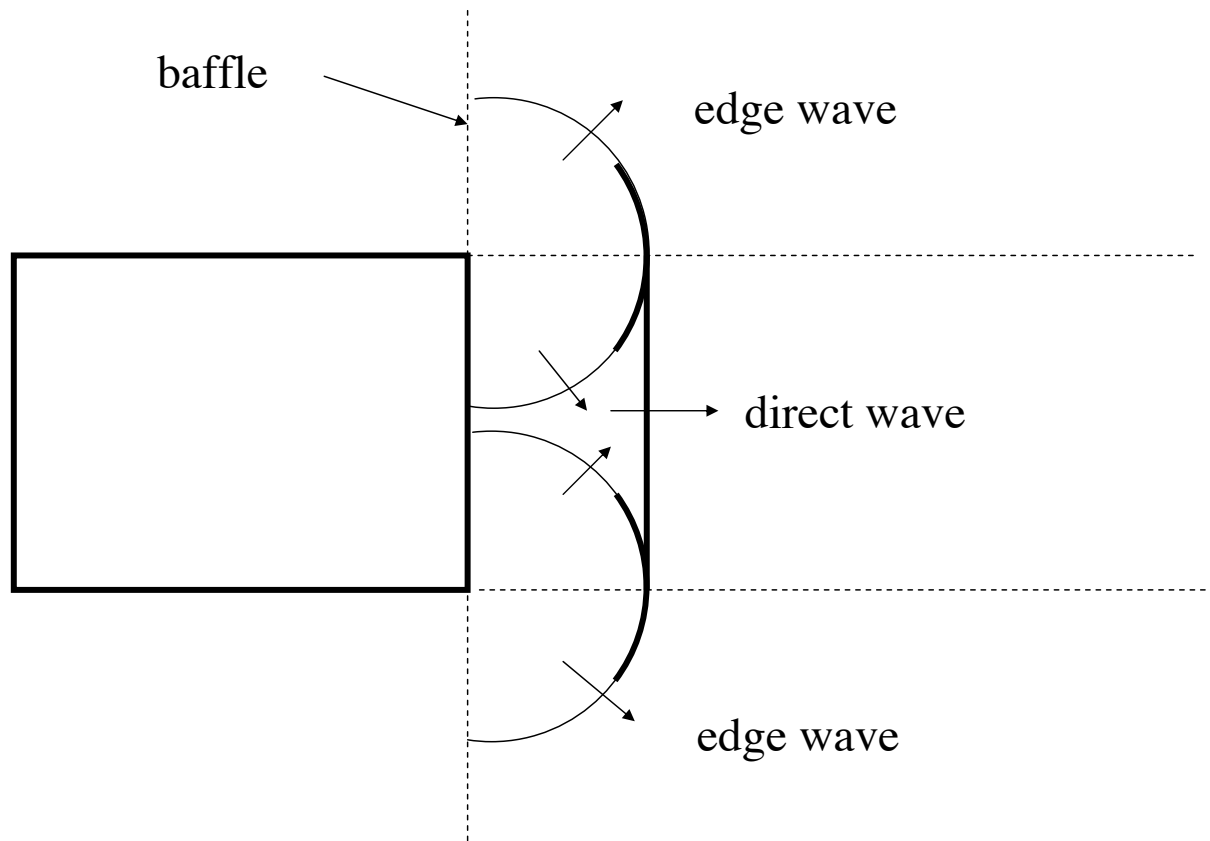


It can be shown that the area element can be written as $dS = r \, dr \, d\phi$

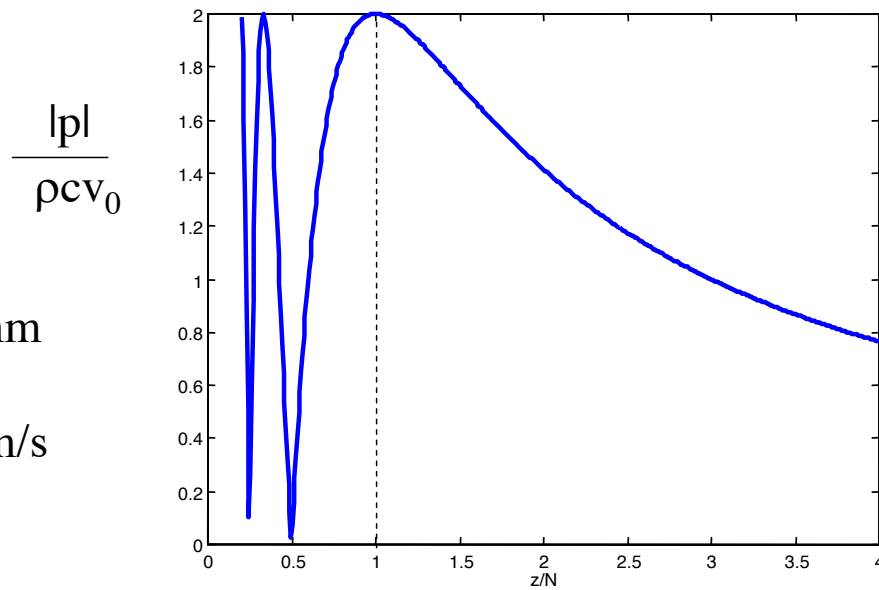
$$p(z, \omega) = \rho c v_0 \left[\exp(ikz) - \exp\left(ik\sqrt{a^2 + z^2}\right) \right]$$



Direct and edge waves as seen for a pulsed transducer



on-axis pressure:



$a = 6.35 \text{ mm}$
 $f = 5 \text{ MHz}$
 $c = 1500 \text{ m/s}$

Near field distance $N = a^2/\lambda$

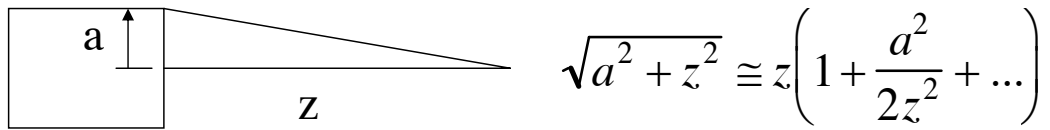


Maxima: $z = N/(2m+1) \quad m = 0, 1, 2, \dots$

Minima: $z = N/2n \quad n = 1, 2, 3, \dots$

Example: for a 5 MHz,
 1/2 in. diameter transducer
 radiating into water
 $N = 5 \text{ in. (approx.)}$

Paraxial approximation : $a/z \ll 1$



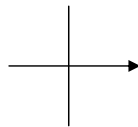
on-axis pressure:

$$p(z, \omega) = \rho c v_0 \exp(ikz) \left[1 - \exp\left(\frac{ika^2}{2z}\right) \right]$$

plane wave

$C_1(a, \omega, z)$

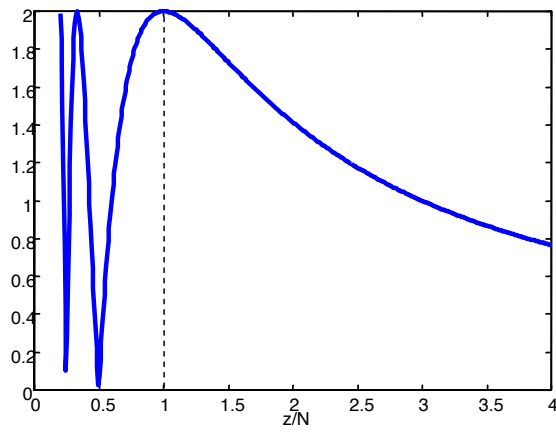
diffraction correction



on-axis pressure:

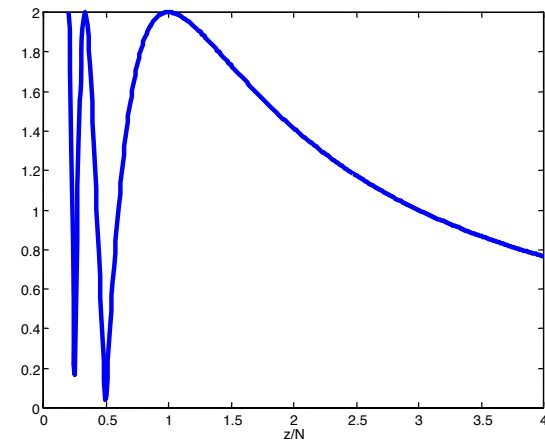
$$\frac{|p|}{\rho c v_0}$$

exact result



$$\frac{|p|}{\rho c v_0}$$

paraxial result



```

function p = on_axis(zN, A,c,F)
% exact on axis pressure from a piston source
%radiating into a fluid. A is radius in mm, c the
%wavespeed of the fluid in m/sec, F the frequency in MHz,
% zN is the distance in the fluid divided by the near field
%distance  $a^2/\lambda$  ( $\lambda$  is the wavelength)
al= 1000*A*F/c; % a/lambda
ka = 2*pi*al; % ka for the transducer
kz = ka*al*zN;
ke = 2*pi*(al^2).*sqrt(zN.^2 + (1/al)^2);
p = exp(i*kz) - exp(i*ke);

```

```

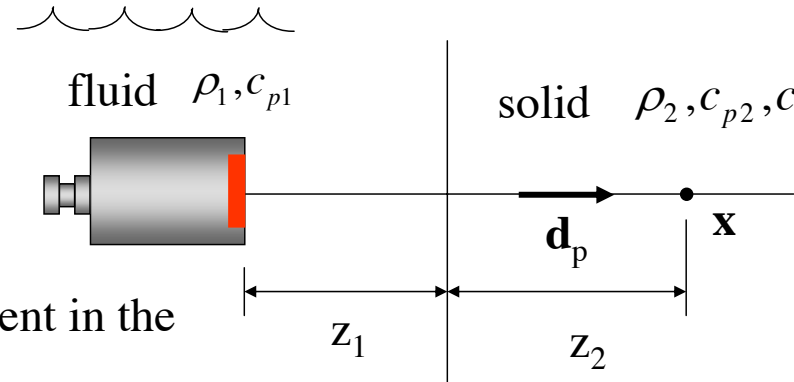
function p = par_on_axis(zN, A,c,F)
% paraxial axis pressure from a piston source
%radiating into a fluid. A is radius in mm, c the
%wavespeed of the fluid in m/sec, F the frequency in MHz,
% zN is the distance in the fluid divided by the near field
%distance  $a^2/\lambda$ 
al= 1000*A*F/c; % a/lambda
ka = 2*pi*al; % ka for the transducer
kz = ka*al*zN;
ke = ka./(2*al.*zN);
p = exp(i*kz).*(1 - exp(i*ke));

```

```
MAT> z = linspace(.2, 4,500);  
MAT> p = on_axis(z,6.35,1500,5);  
MAT> plot(z, abs(p))  
MAT> xlabel('z/N')
```

```
MAT> p = par_on_axis(z, 6.35, 1500, 5);  
MAT> plot(z, abs(p))  
MAT> xlabel('z/N')
```

On-axis response at normal incidence to a plane interface (paraxial approximation)



fluid ρ_1, c_{p1} solid ρ_2, c_{p2}, c_{s2}

displacement in the solid \downarrow

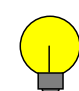
$$\mathbf{u}(\mathbf{x}, \omega) = \frac{v_0}{-i\omega} T_{12}^{P:P} \mathbf{d}_p \exp(ik_{p1}z_1 + k_{p2}z_2) \left[1 - \exp\left(\frac{ik_{p1}a^2}{2\mathcal{Z}}\right) \right]$$

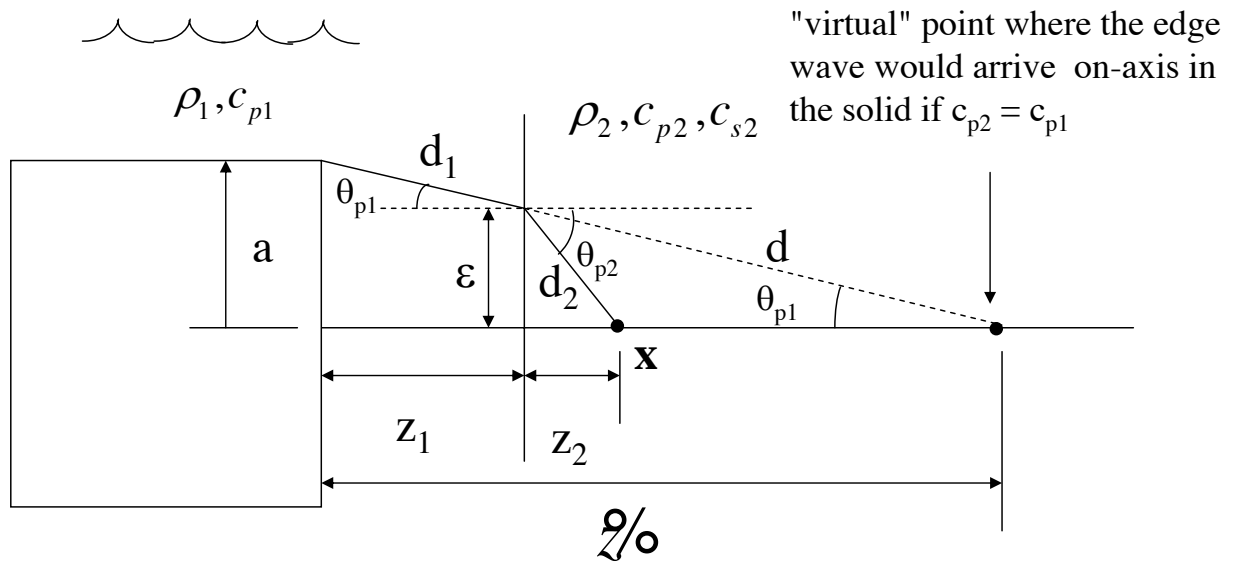
transmission coefficient
(at normal incidence)
(velocity/velocity)

same diffraction correction
expression as for a single fluid

$C(a, \omega, \mathcal{Z})$

$\mathcal{Z} = z_1 + \frac{c_{p2}}{c_{p1}} z_2$





$$\epsilon = d_2 \sin \theta_{p2} = d \sin \theta_{p1} \quad \text{so} \quad d = \frac{\sin \theta_{p2}}{\sin \theta_{p1}} d_2 = \frac{c_{p2}}{c_{p1}} d_2$$

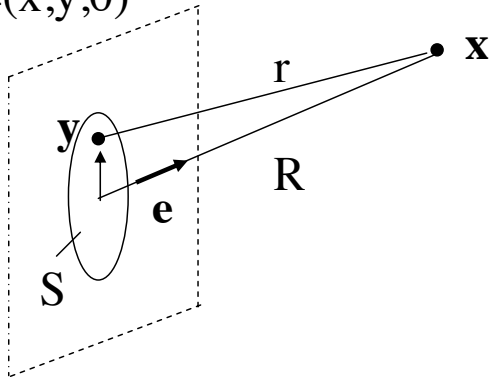
which gives, in the paraxial approximation

$$\frac{a^2}{z/0} \cong \frac{a^2}{d_1 + d} = \frac{a^2}{d_1 + \frac{c_2}{c_1} d_2} \cong \frac{a^2}{z_1 + \frac{c_2}{c_1} z_1}$$

Far-field beam of a planar piston transducer

The far-field is usually defined as $z > 3N$ - also called the "spherical wave region"

$$\mathbf{y} = (x, y, 0)$$



$$\begin{aligned} r &= \sqrt{(\mathbf{x} - \mathbf{y}) \cdot (\mathbf{x} - \mathbf{y})} \\ &= \sqrt{(R\mathbf{e} - \mathbf{y}) \cdot (R\mathbf{e} - \mathbf{y})} \\ &\cong R\sqrt{1 - 2\mathbf{e} \cdot \mathbf{y} / R} \\ &\cong R - \mathbf{e} \cdot \mathbf{y} \end{aligned}$$

$$p(\mathbf{x}, \omega) = \frac{-i\omega\rho v_0}{2\pi} \frac{\exp(ikR)}{R} \int_S \exp(-ik\mathbf{e} \cdot \mathbf{y}) dxdy$$

Define the 2-D spatial Fourier transform of Θ , where $\Theta = \begin{cases} 1 & \text{in } S \\ 0 & \text{otherwise} \end{cases}$

as

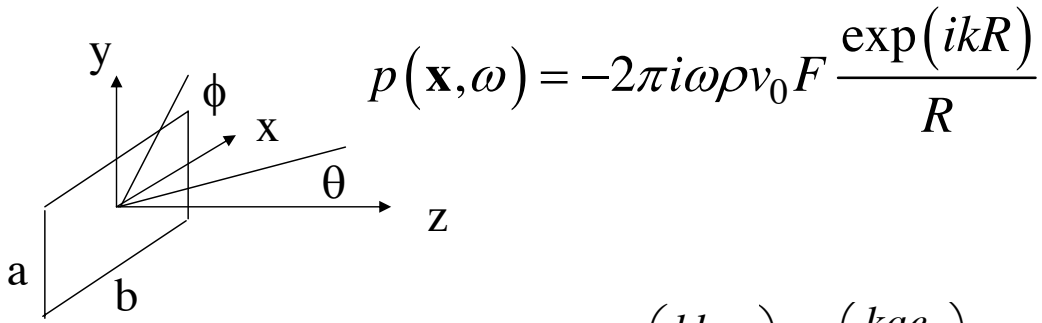
$$F(e_x, e_y, \omega) = \frac{1}{(2\pi)^2} \iint_S \exp(-ip_x x - ip_y y) dx dy \quad p_x = k e_x$$

$$= \frac{1}{(2\pi)^2} \int_{-\infty}^{+\infty} \int_{-\infty}^{+\infty} \Theta(x, y) \exp(-ip_x x - ip_y y) dx dy \quad p_y = k e_y$$

Then the far field pressure can be written as

$$p(\mathbf{x}, \omega) = -2\pi i \omega \rho v_0 \underbrace{F(e_x, e_y, \omega)}_{\text{angular beam profile}} \underbrace{\frac{\exp(ikR)}{R}}_{\text{spherical wave}}$$

Rectangular Piston Transducer



$$p(\mathbf{x}, \omega) = -2\pi i \omega \rho v_0 F \frac{\exp(ikR)}{R}$$

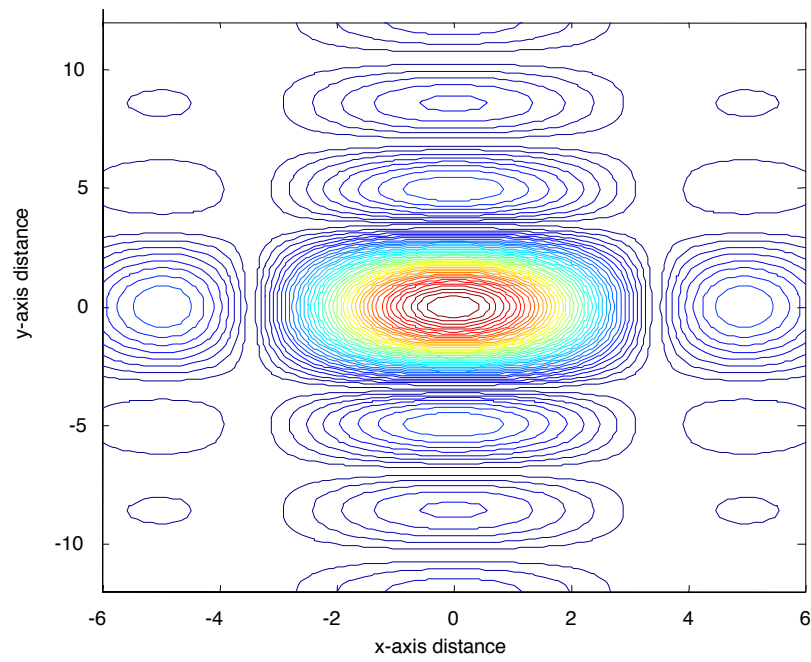
$$F(e_x, e_y, \omega) = \frac{ab}{(2\pi)^2} \frac{\sin\left(\frac{kbe_x}{2}\right) \sin\left(\frac{kae_y}{2}\right)}{\left(\frac{kbe_x}{2}\right) \left(\frac{kae_y}{2}\right)}$$

In spherical coordinates

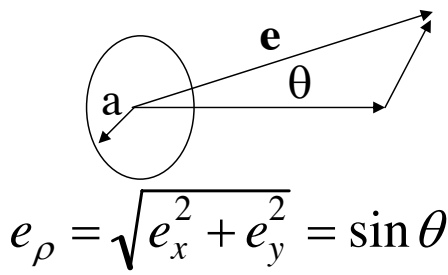
$$e_x = \sin \theta \cos \phi$$

$$e_y = \sin \theta \sin \phi$$

Example far-field pattern of a rectangular transducer

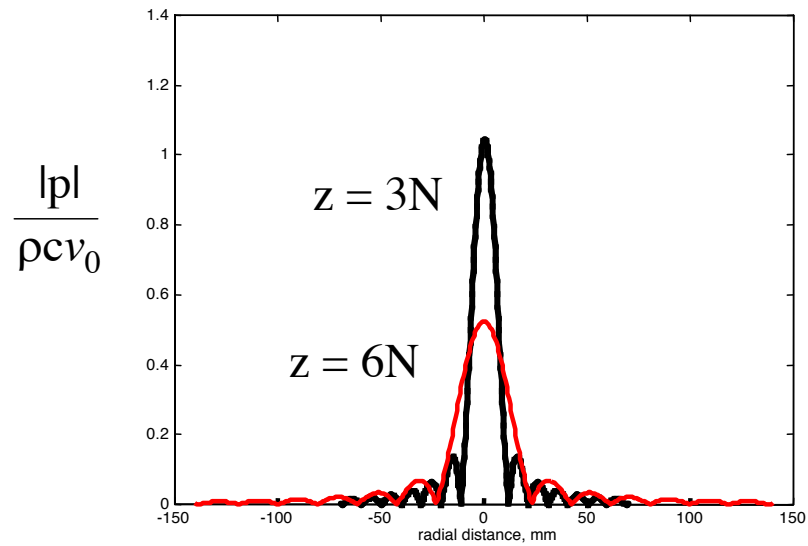


Circular Piston Transducer



$$p(\mathbf{x}, \omega) = -2\pi i \omega \rho v_0 F \frac{\exp(ikR)}{R}$$

$$F(e_x, e_y, \omega) = \frac{a^2}{2\pi} \frac{J_1(ke_\rho a)}{(ke_\rho a)}$$



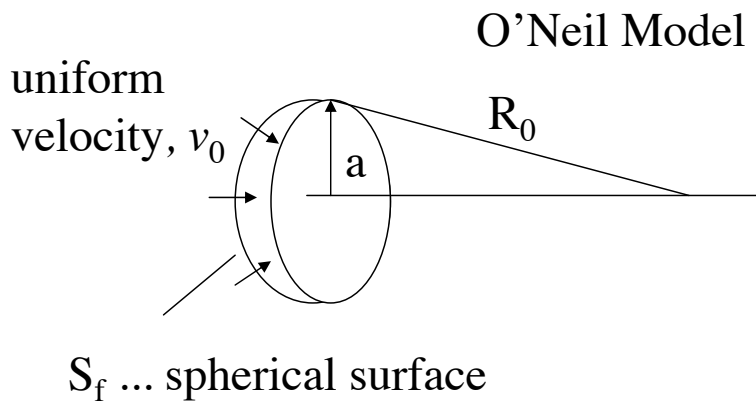
```

function [p, rho] = far_field(ang,A, c, F, RN)
% far_field computes the normalized far field pressure
% for a circular piston (omitting the exp(ikR) phase term)
% A is the radius of the transducer in mm, c the wavespeed
%in m/sec, F the frequency in MHz, and RN is
%the normalized radial distance in near field units.
% rho is the transverse distance (normal to z) in mm
ka = 2*pi*(1000*A*F/c);
al= 1000*A*F/c;
x = ka*sin(ang*pi/180);
rho =RN*(A*al)*sin(ang*pi/180);
p = -i*(ka/(al*RN))*besselj(1,x)./(x+eps*(x ==0));

MAT> ang = linspace(-10, 10,500);
MAT> [p,r] =far_field(ang,6.35,1500,5,3);
MAT> plot(r,abs(p), '--')
MAT> hold on
MAT> [p,r] =far_field(ang,6.35,1500,5,6);
MAT> plot(r,abs(p), 'red')
MAT> xlabel('radial distance, mm')

```

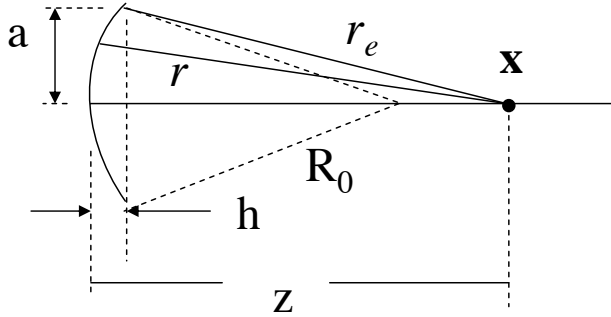
Spherically Focused Piston Transducer Radiating Into a Fluid



$$p(\mathbf{x}, \omega) = \frac{-i\omega\rho v_0}{2\pi} \int_{S_f} \frac{\exp(ikr)}{r} dS(\mathbf{y})$$

For \mathbf{x} on the central axis

$$dS = r \, dr \, d\phi / q_0 \quad q_0 = 1 - z/R_0$$



$$p(\mathbf{x}, \omega) = \frac{\rho c v_0}{q_0} [\exp(ikz) - \exp(ikr_e)]$$

$$r_e = \sqrt{(z - h)^2 + a^2} \quad h = R_0 - \sqrt{R_0^2 - a^2}$$

$a = 6.35 \text{ mm}$

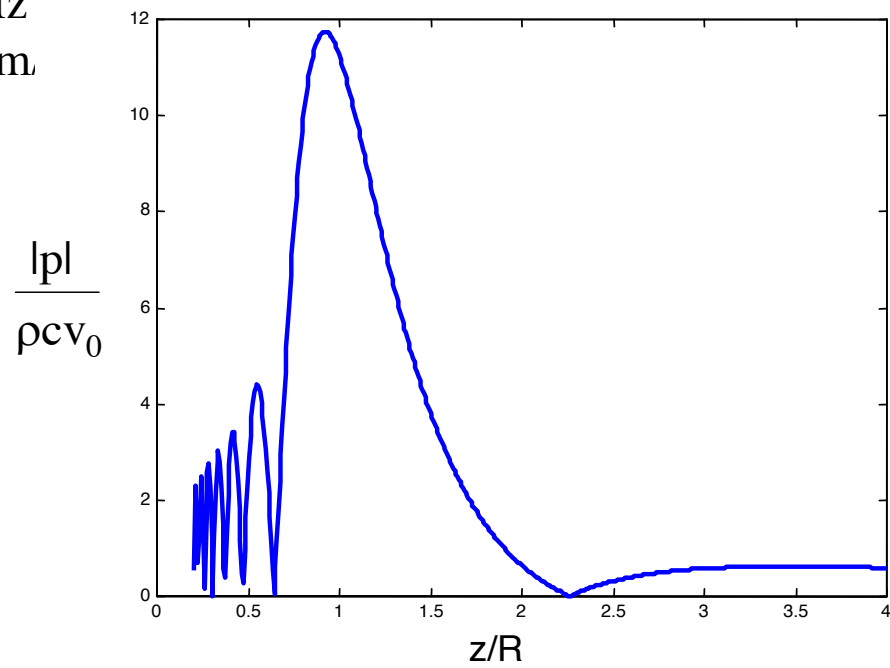
$R_0 = 76.2 \text{ mm}$

$f = 10 \text{ MHz}$

$c = 1480 \text{ m/s}$

on-axis pressure versus z/R_0 :

True focus




```

function p = focused_on_axis(zR, A,c,F,R)
% on axis pressure of a spherically focused probe
% as a function of the normalized distance, zR = z/R
% A, radius of the transducer in mm. R , focal length in mm.
% c, the wave speed in m/sec, and F the frequency in MHz
al=1000*A*F/c;
ka=2*pi*al;
zN=(R/A)*(1/al)*(zR);
kz=ka*al*zN;
kR=2000*pi*F*R/c;
kh=kR-sqrt(kR^2-ka^2);
kre=sqrt((kz-kh).^2+ka^2);
p = (exp(i*kz) -exp(i*kre))./(1-kz./kR);

```

```

MAT> z=linspace(.2,4,500);
MAT> p = focused_on_axis(z,6.35,1480,10,76.2);
MAT> plot(zr,abs(p))
MAT> xlabel('z/R')

```

Paraxial Approximation

$$r_e \cong z + \frac{a^2 q_0}{2z} \qquad q_0 = 1 - z/R_0$$

on-axis pressure:

$$p(z, \omega) = \underbrace{\rho c v_0 \exp(ikz)}_{\text{plane wave}} \underbrace{\left\{ \frac{1}{q_0} \left[1 - \exp\left(\frac{ika^2 q_0}{2z} \right) \right] \right\}}_{\text{diffraction correction}}$$

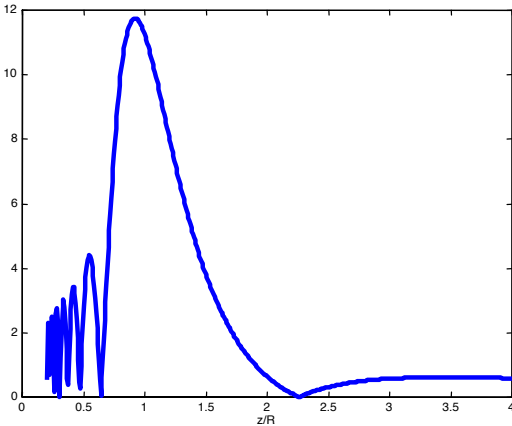
plane wave

diffraction correction

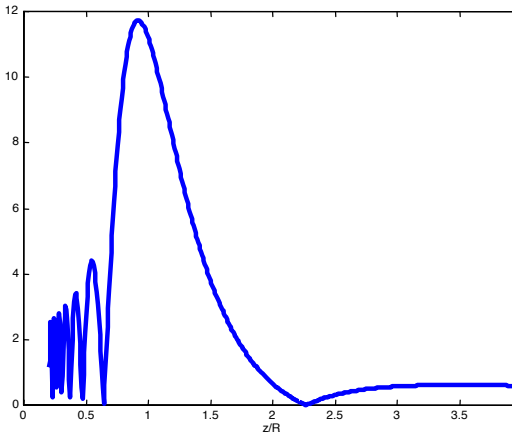
$C_1(a, z, R_0, \omega)$

on-axis pressure

exact $\frac{|p|}{\rho c v}$



paraxial $\frac{|p|}{\rho c v_c}$



```

function p = par_focused_on_axis(zR, A,c,F,R)
% on axis pressure of a spherically focused probe,paraxial approx.
% as a function of the normalized distance, zR = z/R
% A, radius of the transducer in mm. R , focal length in mm.
% c, the wave speed in m/sec, and F the frequency in MHz
al=1000*A*F/c;
ka=2*pi*al;
zN=(R/A)*(1/al)*(zR);
kz=ka*al*zN;
kR=2000*pi*F*R/c;
qo=1-kz./kR;
p = (1-exp(i*ka*(A/R)*qo./(2*zR)))./qo;

```

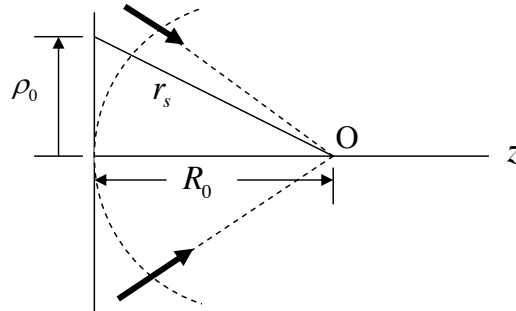
```

MAT> z=linspace(.2,4,500);
MAT> p = par_focused_on_axis(z,6.35,1480,10,76.2);
MAT> plot(zr, abs(p))
MAT> xlabel('z/R')

```

Another way to model focusing (in the paraxial approximation)

suppose on a planar aperture we have a spherical wave propagating (generated by a lens, for example)



then on the aperture we have a phase given approximately in the paraxial approximation ($\rho_0 / R_0 \ll 1$) by

$$\begin{aligned} \exp(-ik[r_s - R_0]) &= \exp\left[-ik\left[\sqrt{\rho_0^2 + R_0^2} - R_0\right]\right] \\ &\cong \exp(-ik\rho_0^2 / 2R_0) \end{aligned}$$

Thus, suppose we use a Rayleigh-Sommerfeld model for a planar transducer and place this phase (in the paraxial approximation) in the integral:

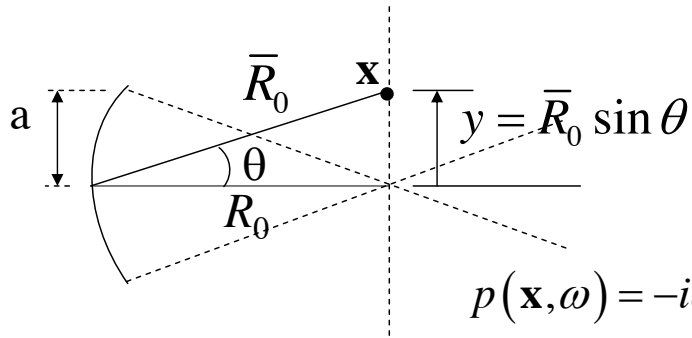
$$p(\mathbf{x}, \omega) = \frac{-i\omega\rho v_0(\omega)}{2\pi} \iint_S \exp(-ik\rho_0^2/2R_0) \frac{\exp(ikr)}{r} dS$$

Using the paraxial approximation and evaluating this integral exactly for \mathbf{x} on the transducer axis gives for a circular transducer of radius a :

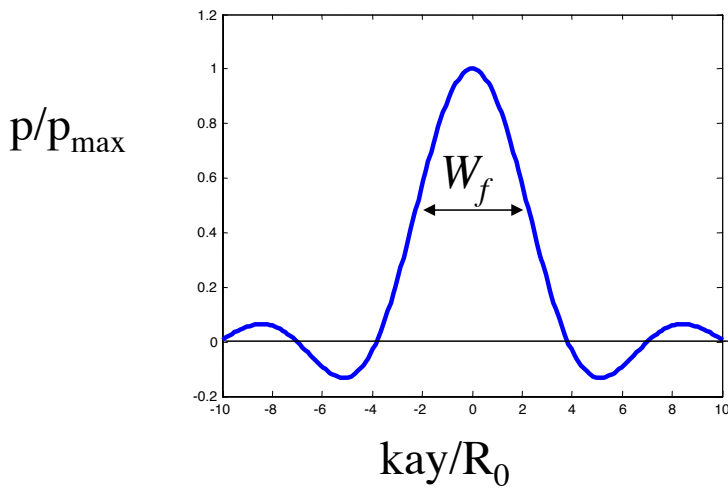
$$p(z, \omega) = \frac{\rho c v_0 \exp(ikz)}{q_0} \left[1 - \exp(ika^2 q_0 / 2z) \right]$$

Similarly, off-axis values will also represent those from a focused transducer

Wave field in the plane at the geometric focus of a spherically focused transducer



$$p(\mathbf{x}, \omega) = -i\omega\rho v_0 a^2 \frac{\exp(ik\bar{R}_0)}{\bar{R}_0} \frac{J_1(kay/\bar{R}_0)}{kay/\bar{R}_0}$$



$$W_f \Big|_{6\text{ dB}} = 4.43 \frac{R_0}{ka} = 1.41 \lambda F$$

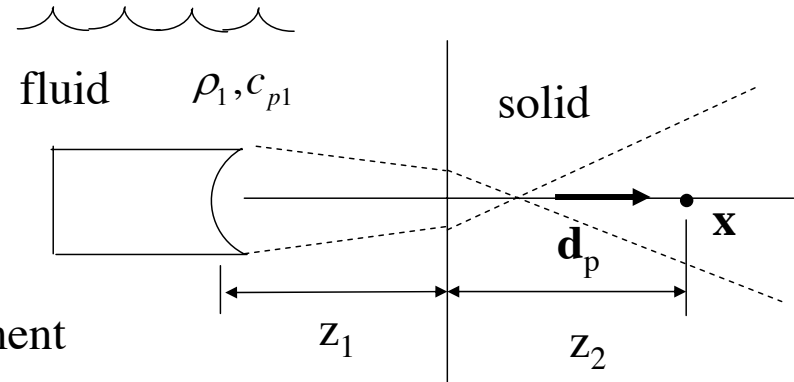


λ ... wavelength

$F = R_0 / 2a$... transducer

F number

On-axis response at normal incidence to an interface (paraxial approximation)



fluid ρ_1, c_{p1} solid ρ_2, c_{p2}, c_{s2}

displacement

$\mathbf{u}(\mathbf{x}, \omega) = \frac{v_0}{-i\omega} T_{12}^{P:P} \mathbf{d}_p \exp(ik_{p1}z_1 + k_{p2}z_2) \left\{ \frac{1}{\mathcal{D}_0} \left[1 - \exp\left(\frac{ik_{p1}a^2 \mathcal{D}_0}{2\mathcal{Z}_0}\right) \right] \right\}$

transmission coefficient
(velocity/velocity)

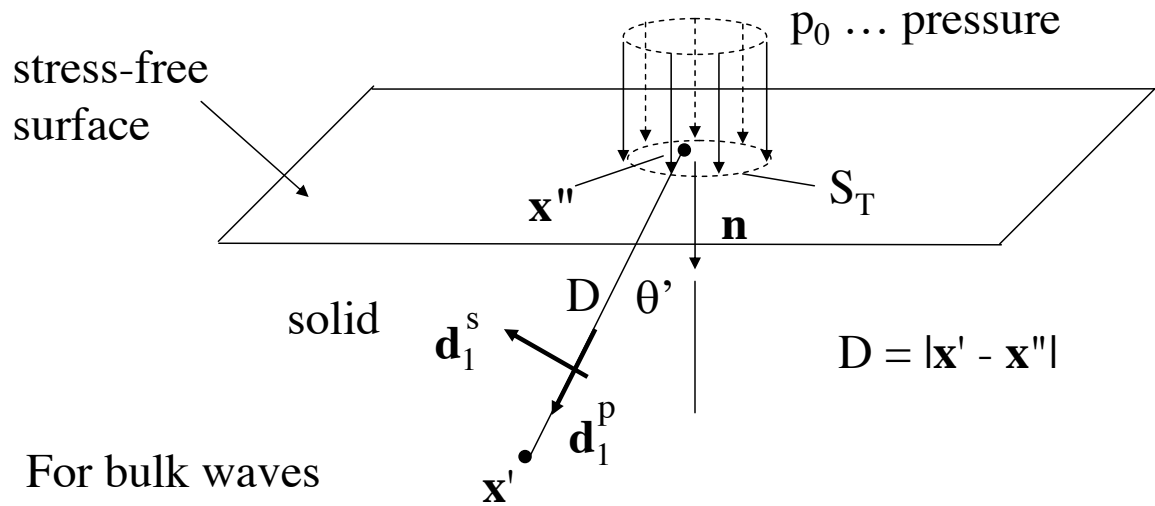
$C(a, \omega, \mathcal{Z}_0)$

same diffraction correction
expression as for a fluid

$\mathcal{Z}_0 = z_1 + \frac{c_{p2}}{c_{p1}} z_2$

$\mathcal{D}_0 = 1 - \frac{\mathcal{Z}_0}{R_0}$

Contact P-wave Transducer Model



$$\mathbf{u}(\mathbf{x}', \omega) = \frac{p_0}{2\pi\rho_1 c_{s1}^2} \int_{S_T} K_s(\theta') \mathbf{d}_1^s \frac{\exp(ik_{s1}D)}{D} dS(\mathbf{x}'')$$

$$+ \frac{p_0}{2\pi\rho_1 c_{p1}^2} \int_{S_T} K_p(\theta') \mathbf{d}_1^p \frac{\exp(ik_{p1}D)}{D} dS(\mathbf{x}'')$$

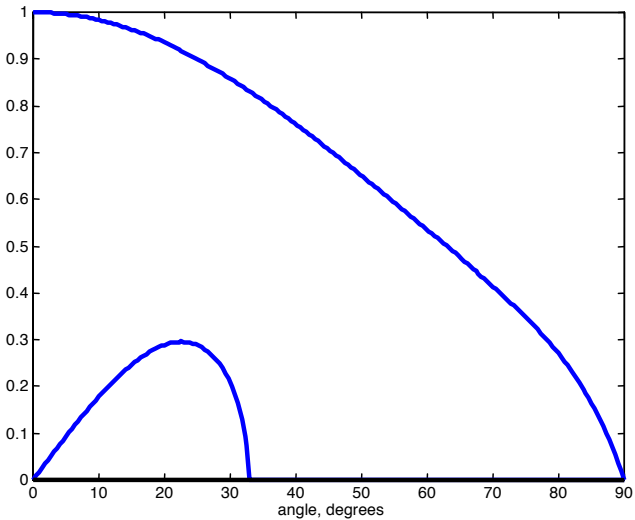
Directivity functions

$$K_p(\theta') = \frac{\cos \theta' \kappa_1^2 \left(\kappa_1^2 / 2 - \sin^2 \theta' \right)}{2 G(\sin \theta')}$$

$$K_s(\theta') = \frac{\kappa_1^3 \cos \theta' \sin \theta' \sqrt{1 - \kappa_1^2 \sin^2 \theta'}}{2 G(\sin \theta')}$$

$$G(x) = \left(x^2 - \kappa_1^2 / 2 \right)^2 + x^2 \sqrt{1 - x^2} \sqrt{\kappa_1^2 - x^2} \qquad \kappa_1 = \frac{c_{p1}}{c_{s1}}$$

K_p, K_s



```

function [kp,ks] = directivity(ang, cp, cs)
% computes the directivity functions for a p-wave contact
%transducer. ang is angle in degrees, cp, cs are p- and s-wave
%speeds
k = cp/cs;
angr = ang*pi/180;
x = sin(angr);
c =cos(angr);
g=(x.^2 -k^2/2).^2 + x.^2.*sqrt(1 - x.^2).*sqrt(k^2 - x.^2);
kp = c.*(k^2).*(k.^2/2 -x.^2)./(2.*g);
ks = (k*x <1).*c.*(k^3).*x.*sqrt(1 - k^2.*x.^2)./(2.*g);

MAT> x = linspace(0,90,200);
MAT> [kp,ks] = directivity(x, 5900, 3200);
MAT> plot(x, kp)
MAT> hold on
MAT> plot(x, ks)
MAT> xlabel('angle, degrees')

```

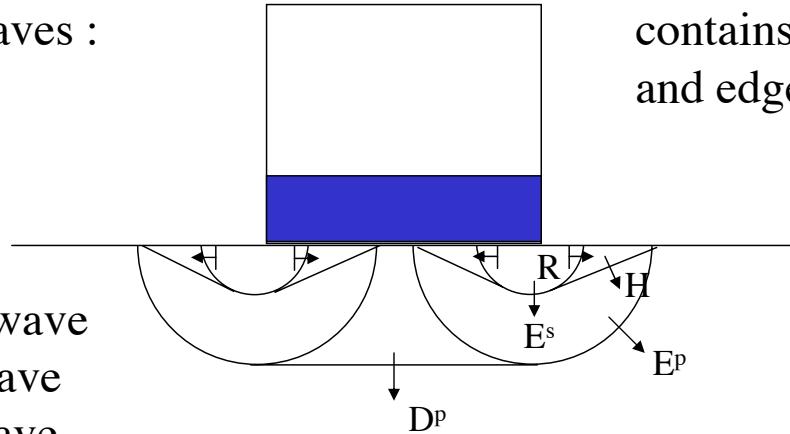
For θ' small $K_p = 1, K_s = 0$

$$\mathbf{u}(\mathbf{x}', \omega) = \frac{p_0 \mathbf{n}}{2\pi \rho_1 c_{p1}^2} \int_{S_T} \frac{\exp(ik_{p1}D)}{D} dS$$

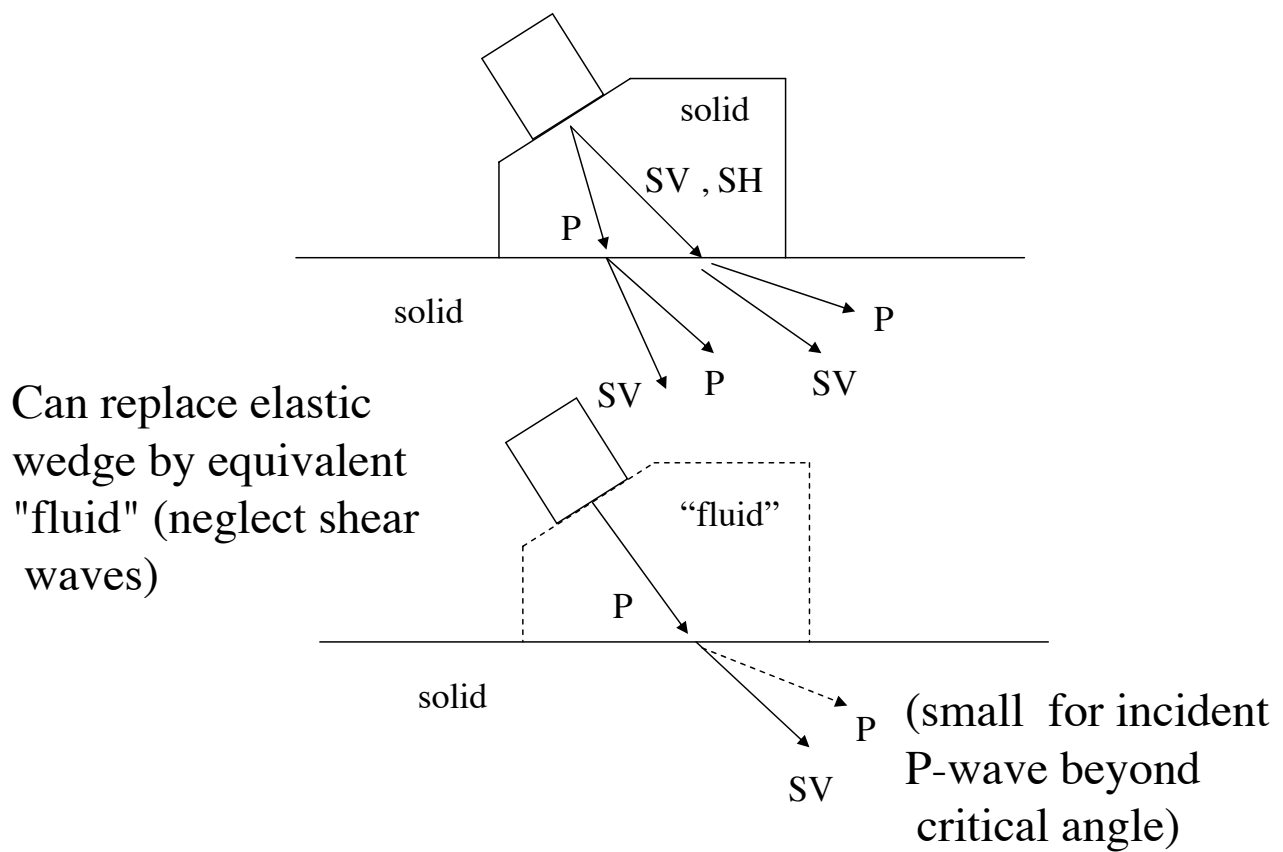
integral
contains direct
and edge P-waves

Full set of waves :

D^p ... Direct P-wave
 E^p ... Edge P-wave
 E^s ... Edge S-wave
 H ... Head wave
 R ... Rayleigh wave



Angle Beam Shear Wave Transducer Model



Ultrasonic Beam Models

Numerically Intense Models

EFIT - Langenberg

Finite Elements - Lord

Boundary Elements - Rizzo

Edge Elements - Schmerr, Lerch

Surface Integral Models

Generalized Point Source - Spies

Rayleigh- Sommerfeld + High Freq. Asymptotics
- Schmerr, Lhemery, others

Line Integral Models

Boundary Diffraction Wave - Schmerr, Lerch

Ultrasonic Beam Models

Other Basis Function Models

Gauss-Hermite Models - Thompson, Gray, Newberry,
Minachi, Margetan

Multi- Gaussian Models

Minachi, Spies, Schmerr and Rudolph, Cervený (Seismology)

Ultrasonic Beam Models

A few references – mostly paraxial models

Lerch, T.P., Schmerr, L.W. and A. Sedov,” Ultrasonic beam models: an edge element approach,” J. Acoust. Soc. Am., 104, 1256-1265, 1998.

Thompson, R. B. and E.F. Lopez,” The effects of focusing and refraction on Gaussian ultrasonic beams,” J. Nondestr. Eval., 4, 107-123, 1984.

Newberry, B.P. and R.B. Thompson,” A paraxial theory for the propagation of ultrasonic beams in anisotropic solids,” J. Acoust. Soc. Am., 85, 2290-2300, 1989.

Schmerr, L.W., Rudolph, M., and A. Sedov,” Modeling ultrasonic transducer wave fields for general complex geometries and anisotropic materials,” **Review of Progress in Quantitative Nondestructive Evaluation**, D. O. Thompson and D.E. Chimenti, Eds., Plenum Press, New York, 19A, 953-960, 2000.

Ultrasonic Beam Models

Schmerr, L. W., **Fundamentals of Ultrasonic Nondestructive Evaluation**, Plenum Press, New York, 1998.

Spies, M., and M. Kroning," Ultrasonic inspection of inhomogeneous welds simulated by Gaussian beam superposition," **Review of Progress in Quantitative Nondestructive Evaluation**, D. O. Thompson and D.E. Chimenti, Eds., Plenum Press, New York, 18A, 1107-1114, 1999.

Minachi, A., Margetan, F.J., and R.B. Thompson," Reconstruction of a piston transducer beam using multi-Gaussian beams (MGB) and its applications," **Review of Progress in Quantitative Nondestructive Evaluation**, D. O. Thompson and D.E. Chimenti, Eds., Plenum Press, New York, 17A, 907-914, 1989.

Gengembre, N. and A Lhemery, " Calculation of wide band ultrasonic fields radiated by water-coupled transducers into heterogeneous media," **Review of Progress in Quantitative Nondestructive Evaluation**, D. O. Thompson and D.E. Chimenti, Eds., Plenum Press, New York, 18A, 1107-1131, 1999.